Reconnection at the dayside magnetopause: Comparisons of global MHD simulation results with Cluster and Double Star observations

J Berchem, Aurélie Marchaudon, M Dunlop, C P Escoubet, J M Bosqued, H Reme, I Dandouras, A Balogh, E Lucek, C Carr, et al.

JOURNAL OF GEOPHYSICAL RESEARCH, VOL. 113, A07S12, doi:10.1029/2007JA012743, 2008

Reconnection at the dayside magnetopause: Comparisons of global MHD simulation results with Cluster and Double Star observations

J. Berchem,[1] A. Marchaudon,[2] M. Dunlop,[3] C. P. Escoubet,[4] J. M. Bosqued,[5] H. Reme,[5] I. Dandouras,[5] A. Balogh,[6] E. Lucek,[6] C. Carr,[6] and Z. Pu[7]

Received 21 August 2007; revised 22 November 2007; accepted 22 January 2008; published 8 May 2008.

[1] This study uses two conjunctions between Cluster and Double Star TC-1 spacecraft together with global magnetohydrodynamic (MHD) simulations to investigate the large-scale configuration of magnetic reconnection at the dayside magnetopause. Both events involve southward interplanetary magnetic fields with significant B_y components. The first event occurred on 8 May 2004, while both spacecraft were exploring the dawn flank of the magnetosphere; TC-1 was skimming the magnetopause whereas Cluster was exploring higher latitudes. Results from a global MHD simulation show the formation of an equatorial merging line in the morning sector and suggest that the three-dimensional geometry of the merging region is mostly a radial juxtaposition of planes displaying *X*-type reconnection geometries. The second conjunction was on 6 April 2004. During this event, Cluster was located at high latitudes and close to the noon-midnight meridian, while TC-1 was exploring the dawnside at low latitudes. Analysis of the simulation reveals that both antiparallel and component merging occurred simultaneously. Three-dimensional rendering of the parallel electric field indicates that component merging initiated in the subsolar magnetopause. Simulation runs carried out using different parameters in the model suggest that the spread of the merging region depends on the local resistivity. The subsolar-merging region grows with increasing resistivity values and becomes patchy when a resistivity threshold is used. However, the region of component merging appears to remain spatially constrained to the subsolar region where stronger parallel electric fields occur and no clear connection with the antiparallel-merging regions is found for the range of parameters surveyed.

Citation: Berchem, J., et al. (2008), Reconnection at the dayside magnetopause: Comparisons of global MHD simulation results with Cluster and Double Star observations, *J. Geophys. Res.*, *113*, A07S12, doi:10.1029/2007JA012743.

1. Introduction

[2] Although magnetic reconnection is well known, the large-scale process by which the IMF merges with the geomagnetic field at the dayside magnetospheric boundary has proven difficult to assess. For example, it is still unknown whether merging occurs preferentially in the subsolar region of the magnetopause through component merging during southward IMF [e.g., *Sonnerup*, 1970, 1974; *Cowley*, 1973, 1974a, 1974b, 1976; *Gonzalez and Mozer*, 1974; *Hill*, 1975] or, alternatively, the presence of even a small east-west IMF component forces the merging region to split into two branches away from the subsolar region, as predicted by the antiparallel merging model [*Crooker*, 1979; *Luhmann et al.*, 1984]. In particular, it has been difficult to determine the 3-D properties and consequences of the merging process. Most of the community still relies on 2-D pictures and phenomenological models to test for the occurrence of magnetic reconnection.

[3] Despite the limitations of available observations, a considerable amount of information has been collected. However, neither the component-merging model nor the antiparallel-merging model alone provides a comprehensive solution. For example, most of the low-latitude observations of plasma flow reversals associated with reconnection during periods of predominantly southward IMF were found to be consistent with the component merging model [*Sonnerup et al.*, 1981; *Paschmann et al.*, 1986; *Gosling et al.*, 1990; *Phan et al.*, 1996]. For northward IMF the situation is more ambiguous. While identification of reconnection signatures

[1]Institute of Geophysics and Planetary Physics, University of California Los Angeles, Los Angeles, California, USA.
[2]Laboratoire de Physique et Chimie de l'Environnement, CNRS, Orleans, France.
[3]Rutherford Appleton Laboratory, Didcot, UK.
[4]European Space Research and Technology Centre, European Space Agency, Noordwijk, Netherlands.
[5]Centre d'Etude Spatiale des Rayonnements, UMR 5187, CNRS, Toulouse, France.
[6]Blackett Laboratory, Imperial College, London, UK.
[7]School of Earth and Space Sciences, Peking University, Beijing, China.

0148-0227/08/2007JA012743$09.00

poleward of the cusps supports the antiparallel merging model [e.g., *Kessel et al.*, 1996; *Russell et al.*, 1998], there are also observations of signatures in particle distributions that indicate reconnection can take place equatorward of the cusp and thus be consistent with component merging [*Onsager and Fuselier*, 1994; *Fuselier et al.*, 1997; *Chandler et al.*, 1999].

[4] It has also been difficult to resolve the complex signatures of the merging region's global topology in the observed ionospheric precipitation patterns. One of the major stumbling blocks in the effort to do so has been attaining an accurate mapping of ionospheric emissions to magnetopause locations with accelerated particles. Although observation-based magnetic field models [e.g., *Tsyganenko*, 1995] have been invaluable for mapping the merging region for evaluating different hypotheses of the merging geometry, their use has been more equivocal in interpreting actual observations. A low-velocity cutoff technique for precipitating and mirroring magnetosheath ions in the cusp was developed to calculate the distance to the reconnection line [*Fuselier et al.*, 2000a, 2000b; *Trattner et al.*, 2004, 2005]. The distance found is subsequently traced back to the magnetopause using Tsyganenko's model, which calculates the shear angle between the magnetospheric field and the draped IMF field. Recently *Trattner et al.* [2004] used this method to conduct statistical studies of reconnection during northward IMF conditions. They found that antiparallel and component merging were approximately equally likely to occur. *Trattner et al.* [2004] also remarked that reconnection was most likely to extend from small antiparallel reconnection sites to regions where the magnetic fields are no longer strictly antiparallel, in effect suggesting that antiparallel and component reconnection could plausibly occur simultaneously. However, their latest study, on the basis of 130 events with southward IMF, reveals that in general magnetic reconnection occurs along an extended line across the dayside magnetopause, which is consistent with the tilted *X*-line predicted by the component-merging model [*Trattner et al.*, 2007].

[5] Early semiglobal MHD simulation models for southward IMF suggested that reconnection occurs predominantly in the subsolar region [e.g., *Sato et al.*, 1986], which supports the component-merging model. However, numerical algorithms of these simulations were too diffusive to support a detailed analysis of the topology of the reconnection region. Results from subsequent global studies were, for the most part, consistent with antiparallel merging, though the geometry of the merging region was usually treated only peripherally. One notable result from these studies was the identification of a region of weak magnetic field strength for duskward IMF. This region was found to run tailward along the high-latitude magnetopause flanks from one dayside cusp to the other and to contain the magnetic separator line. It was referred to as the magnetospheric sash and found to be consistent with the prediction of merging site loci, as determined from the antiparallel-merging model [*White et al.*, 1998; *Maynard et al.*, 2001]. Similarly, earlier global MHD simulations [e.g., *Fedder et al.*, 1995; *Berchem et al.*, 1998b; *Berchem*, 2002] produced localized regions of the dayside magnetopause marked by high-beta plasma values that were also consistent with antiparallel merging. Studies of lobe-cell convection using the global LFM code also supported the concept of antiparallel merging [*Crooker et al.*, 1998]. Later *Siscoe et al.* [2001], using results from a global MHD simulation, computed the distribution of the parallel electric field along the topological separator line between open and closed field lines. They concluded that reconnection behavior is more component-like for southward IMF conditions and more antiparallel-like for northward IMF. In discussing the global reconnection rate found by integrating the parallel electric field along the separator, *Siscoe et al.* [2001] mentioned that it appeared to be controlled by global physics rather than local processes.

[6] Recently *Moore et al.* [2002] used the component-merging concept and *Tsyganenko and Stern*'s [1996] magnetic field model to determine where reconnection occurs for different clock angles of the IMF. The technique employed was to choose points with the largest reconnecting component and integrate the local *X*-line from that point, tracing it wherever it led, much like tracing streamlines of a vector field. They found reconnection occurred in the subsolar region of the magnetopause for virtually all cases of southward IMF, with more complex patterns developing during northerly orientation, including the formation of separate merging lines both poleward and equatorward of the cusps. *Dorelli et al.* [2004] used global MHD simulations to demonstrate that under generic northward IMF conditions, magnetic reconnection occurs at the subsolar magnetopause via a flux pileup mechanism, though other modes of reconnection may take place in stationary reconnection sites [e.g., *Siscoe et al.*, 2002]. These results are in conflict with the component-merging model [e.g., *Sonnerup*, 1974] and most of the current interpretations of global simulation results, which predict that subsolar reconnection is limited by the angle between the IMF and the magnetospheric field. For example, *Moore et al.* [2002] predicted that subsolar reconnection shut down completely during exactly northward IMF. In a recent paper, *Dorelli et al.* [2007] examined three-dimensional reconnection in detail and argued that, even under northward IMF conditions, reconnection displays features of both antiparallel reconnection near the cusp nulls and component reconnection near the subsolar separator line.

[7] To summarize, determining the large-scale topology of the reconnection processes occurring at the dayside magnetopause is one of the most critical unresolved issues of magnetospheric physics. Neither the component-merging model nor the antiparallel-merging model alone is sufficient for reaching a comprehensive solution. While potential sites of antiparallel merging are fairly predictable for a specific orientation of the IMF, it is unclear what governs the location of component merging. For some years it has generally been assumed that component merging begins at the subsolar magnetopause, but this remains to be proven. It is also not known how far the merging line extends from that region in forming a tilted neutral line [*Sonnerup*, 1974; *Cowley*, 1976; *Sonnerup et al.*, 1981; *Cowley and Owen*, 1989; *Fuselier et al.*, 2002a, 2002b]. Although microscopic studies indicate that component reconnection can occur almost anywhere, the paucity of in situ observations of reconnection suggests that the occurrence of merging is limited to very specific regions of the dayside magnetopause. This suggests that macroscopic factors might exert

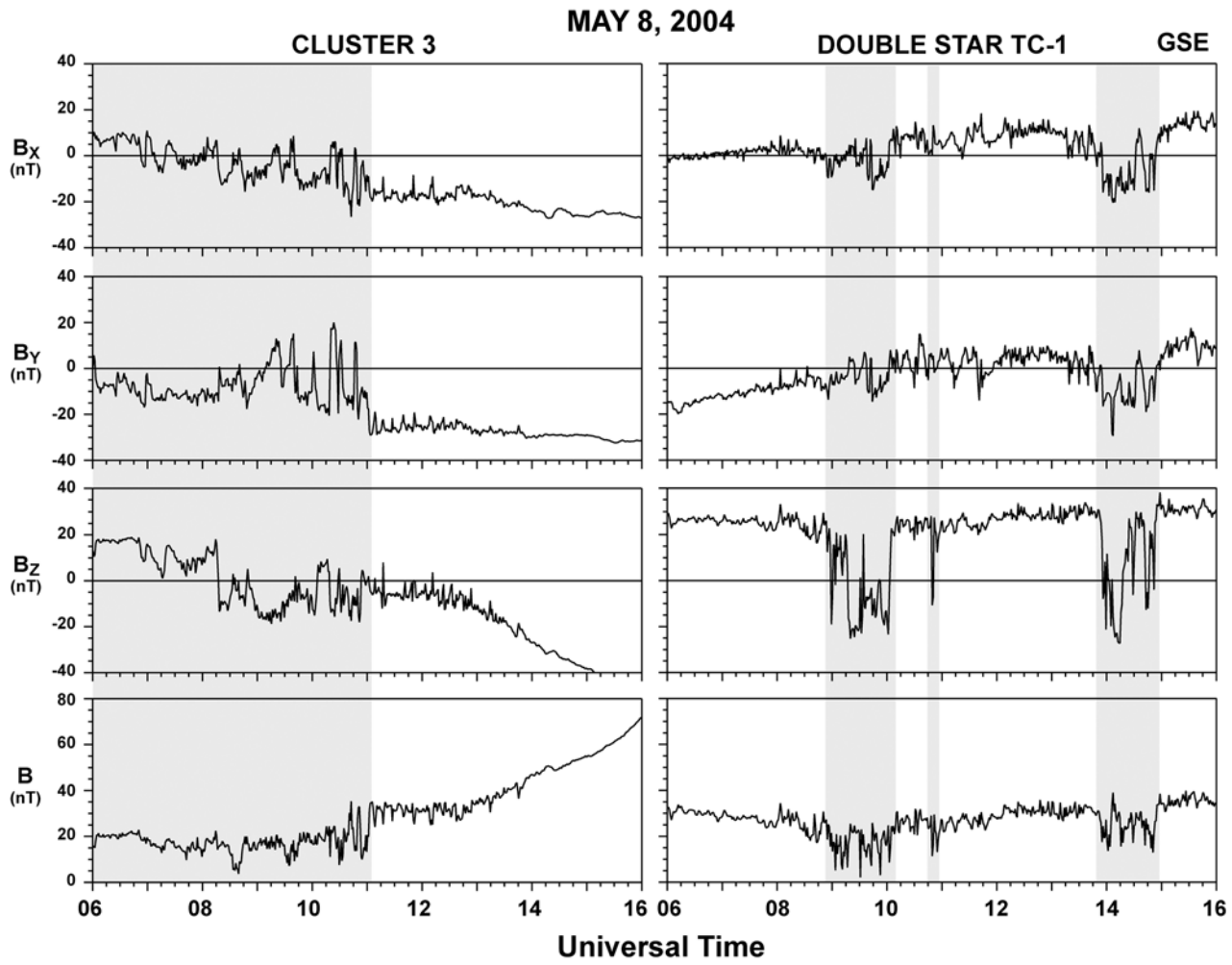

Figure 1. Magnetic field measured by the (left) Cluster 3 and (right) TC-1 spacecraft on 8 May 2004. Data are displayed in GSE coordinates. The Cluster spacecraft entered the magnetopause boundary layer at around 11:00 UT after a series of partial magnetopause crossings and remained close to the magnetopause boundary of the Southern Hemisphere until about 13:00 UT. TC-1 was primarily skimming the magnetospheric boundary but made three major incursions into the magnetosheath between 08:50–10:03 UT, 10:48–10:50 UT, and 13:45–15:00 UT.

greater influence in locations where the IMF reconnects with the geomagnetic field than do local microscopic conditions [e.g., *Siscoe et al.*, 2001].

[8] Section 2 presents the first of this paper's two studies; the studies used synoptic measurements from Cluster and Double Star TC-1 and the results of global MHD simulations in an effort to determine the global topology of the dayside-merging regions. The first conjunction event occurred on 8 May 2004, and we focus on a time interval during which the IMF interacting with the magnetosphere was predominantly southward. After a brief description of the observations, we examine the topology of the magnetic field as calculated from the global simulations and identify the merging regions. Section 3 presents a second study using a conjunction that occurred on 6 April 2004. During that event the IMF was also southward but had a stronger B_y component than during the 8 May case. We use isosurfaces of the plasma beta and the parallel electric field together with field-line tracings from the simulations to establish the global topology of reconnection during the event. Next, in section 4, we compare and contrast the different global configurations of the dayside magnetosphere inferred from the simulations and discuss the topology of the merging regions found in the simulations. Section 5 concludes the paper with a summary of the results.

2. The 8 May 2004 Event

[9] The first conjunction event examined in this paper occurred on 8 May 2004. During that time the Cluster [*Escoubet et al.*, 2001] and TC-1 spacecraft [*Liu et al.*, 2005] were exploring the same magnetic local time (MLT) of the dawn flank of the magnetosphere. Cluster was reentering the magnetosphere at high latitudes on a mainly dawn-dusk trajectory in the Southern Hemisphere while TC-1, near its apogee, was skimming the equatorial mag-

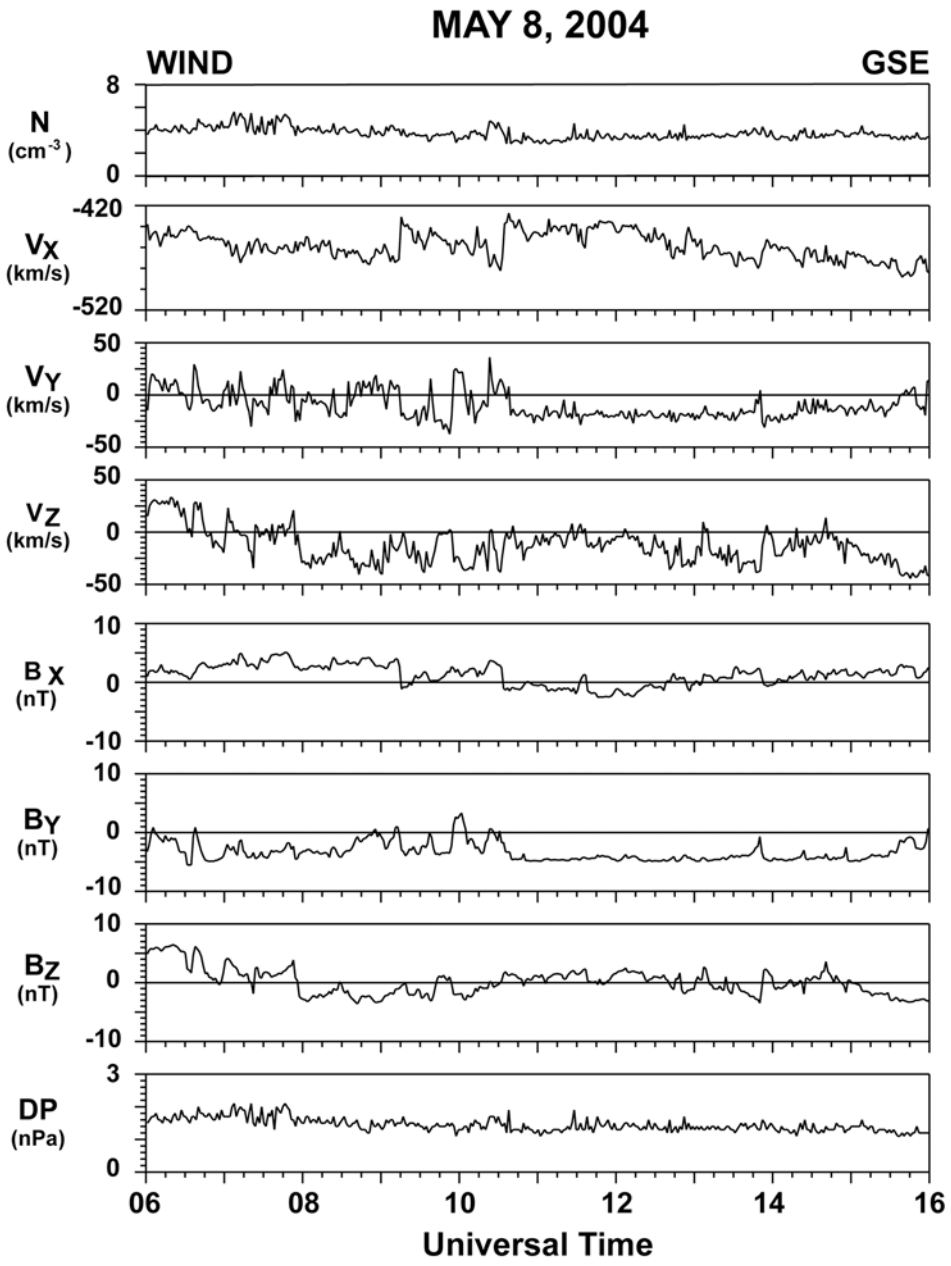

Figure 2. Magnetic field measurements from the Wind spacecraft for 8 May 2004. There is a lag of about 21 min between Wind and Cluster measurements.

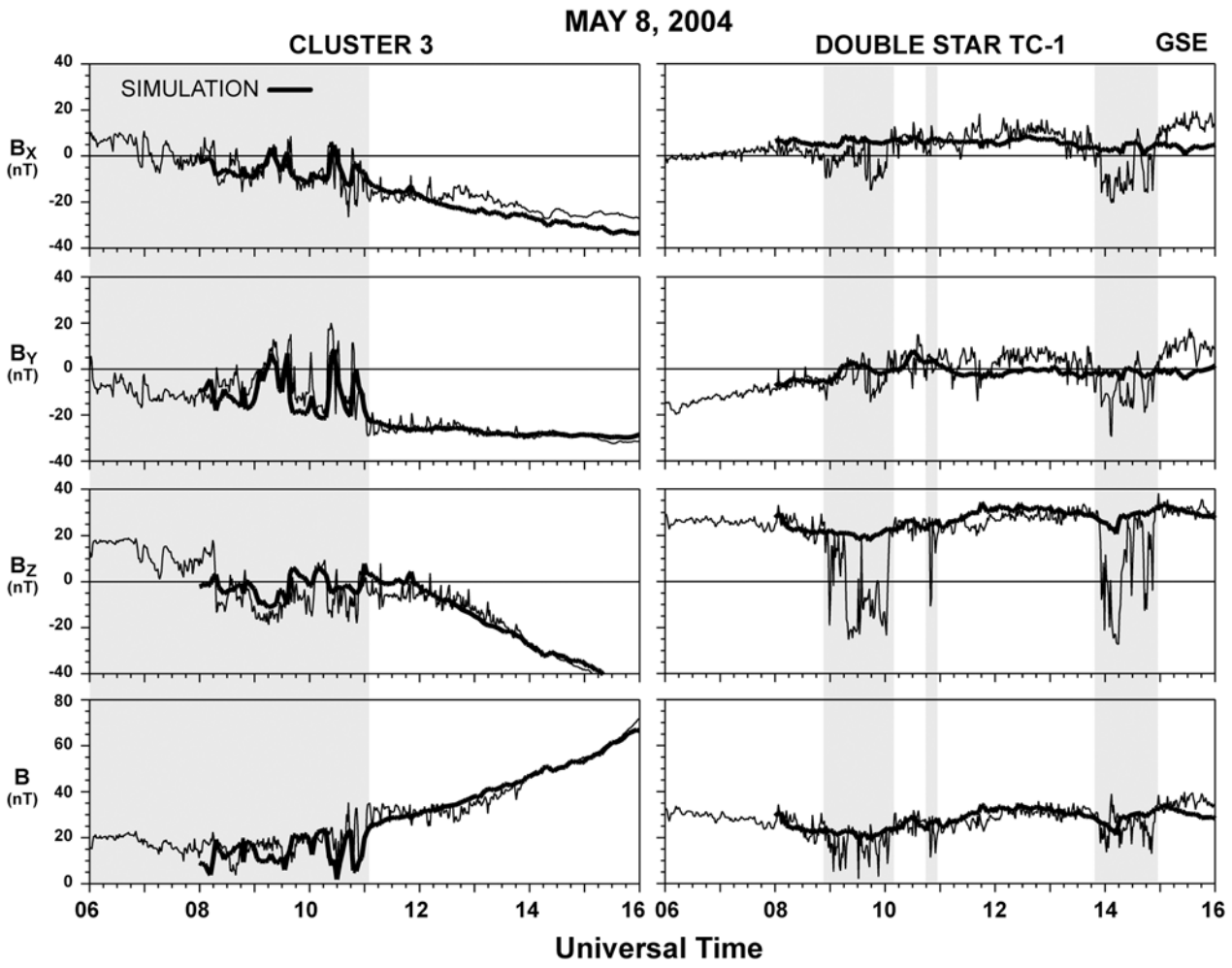

Figure 3. Thick traces show the superposition of the simulation data streams over a time series of the magnetic field measured at (left) Cluster and (right) TC-1 on 8 May 2004. The magnetopause crossings and trends in the magnetospheric field observed by Cluster are well reproduced by the simulation. The computational grid is not fine enough for the simulation to reproduce small-amplitude oscillations or the sharp gradients observed by the spacecraft as they cross the magnetopause.

netopause. The magnetic field measured by the FluxGate Magnetometers (FGM) onboard the Cluster 3 [*Balogh et al.*, 2001] and TC-1 [*Carr et al.*, 2005] spacecraft during the 08:00–16:00 UT time interval of the conjunction are shown in Figure 1. The geocentric solar ecliptic (GSE) coordinate system is used throughout the paper to display spacecraft measurements and simulation results. Magnetic field measurements displayed in Figure 1 indicate the Cluster spacecraft entered the magnetopause boundary layer at around 11:00 UT [$x_{GSE} = 0.13$; $y_{GSE} = -9.36$; $z_{GSE} = -10.20\ R_E$] after a series of partial magnetopause crossings. The spacecraft remained close to the magnetospheric boundary of the Southern Hemisphere until about 13:00 UT.

[10] During the conjunction, TC-1 was primarily skimming the equatorial region of the dawn magnetospheric boundary [$x_{GSE} \approx 3$; $y_{GSE} \approx -12$; $z_{GSE} \approx -1\ R_E$], but made three major incursions into the magnetosheath between 08:50–10:03 UT, 10:48–10:50 UT, and 13:45–15:00 UT. These incursions were marked by multiple magnetopause crossings. *Marchaudon et al.* [2005] carried out a comprehensive study of Cluster and TC-1 high-resolution magnetic field and plasma measurements and concluded that numerous Flux Transfer Events (FTEs) [*Russell and Elphic*, 1978] occurred throughout the conjunction period between the spacecraft. These FTEs appear as clearly noticeable small amplitude oscillations in the low-resolution data shown in Figure 1. The very clear signatures and finite transverse sizes of the FTEs observed by TC-1 and Cluster suggest that sporadic reconnection occurred during this event. *Marchaudon et al.* [2005] used the polarities of the FTEs' signatures [e.g., *Berchem and Russell*, 1984], along the magnetic field component normal to the local magnetopause surface, to infer that the FTEs were moving southward and tailward from the reconnection site, and thus that the reconnection region was located northward of TC-1 and Cluster.

[11] Figure 2 shows the Wind plasma [*Ogilvie et al.*, 1995] and magnetic field [*Lepping et al.*, 1995] measurements used as input to the global MHD simulation carried out for this study. Comparing Cluster magnetic field measurements with solar wind data from the Wind spacecraft [$x_{GSE} = 98.0$; $y_{GSE} = -30.9$; $z_{GSE} = -10.1\ R_E$] revealed a

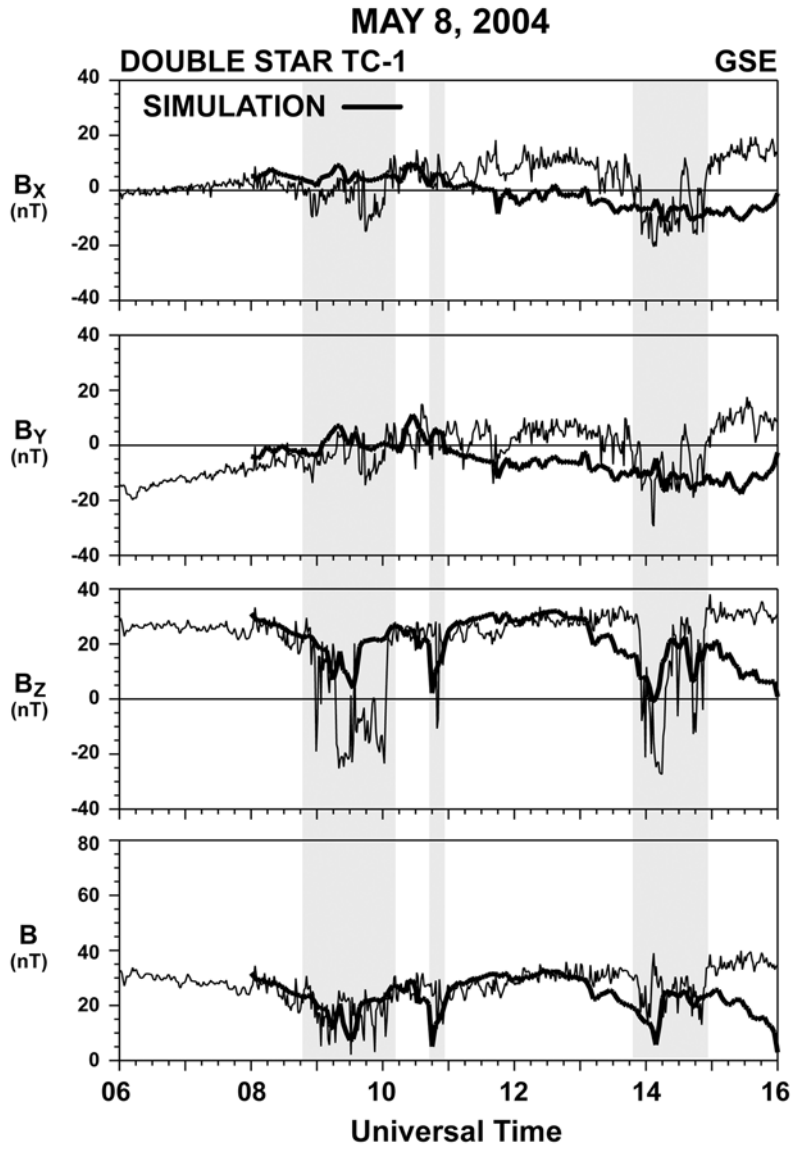

Figure 4. Thick traces show the superposition of the simulation data streams over the magnetic field measured at TC-1 on 8 May 2004. The location of the virtual TC-1 spacecraft has been shifted toward dawn by 0.5 R_E. This shift significantly improves the agreement between the simulation results and the observations shown in Figure 3.

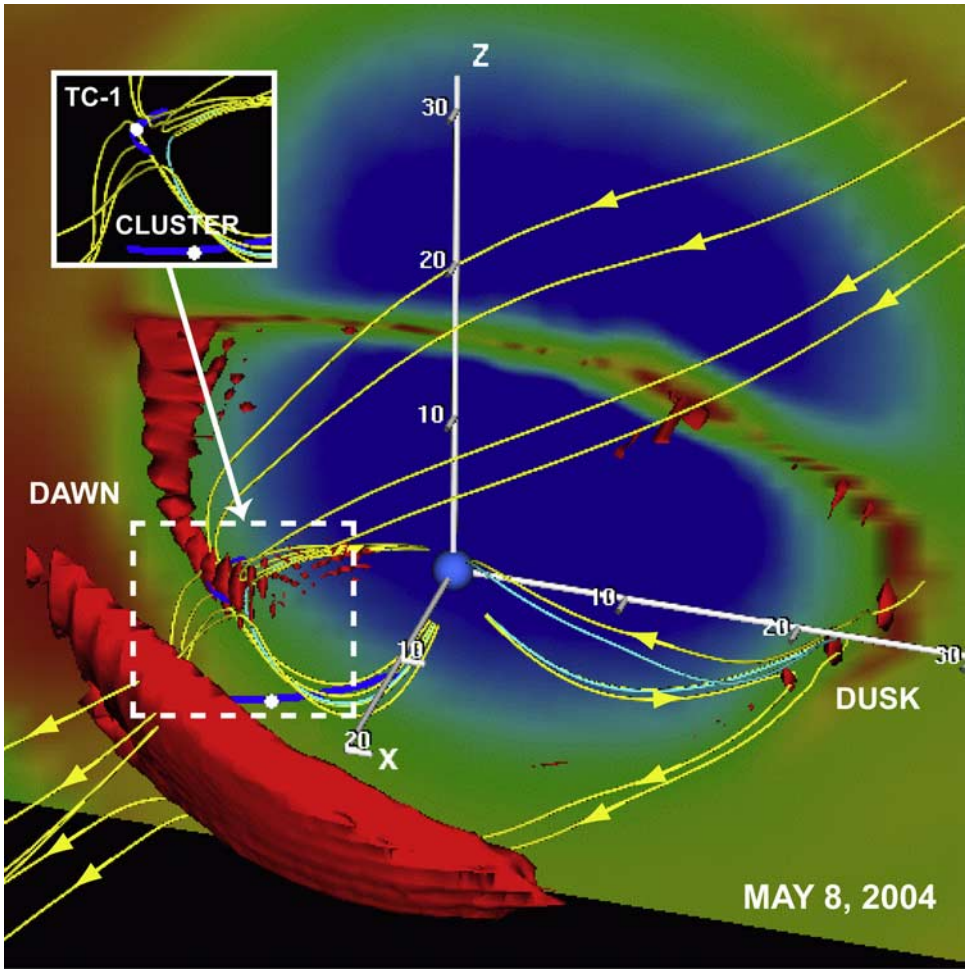

Figure 5. Composite picture of two- and three-dimensional renderings of the dayside magnetosphere obtained using the simulation results for time 10:03 UT on 8 May 2004. The dayside magnetopause is viewed from 14:00 LT. The backdrop of the picture is a two-dimensional cross section (*Y-Z* plane) of the magnetotail taken at $x = -10\ R_E$ and shows color contours of the plasma beta. A three-dimensional isosurface of plasma beta (=100) completes the picture with the same color coding as that of the cross section contours. Unconnected, open, and closed field lines are shown in red, yellow, and turquoise, respectively. The inset displays the dawnside region hided from view by the isosurface. Cluster and TC-1 trajectories during the 06:00–16:00 UT time interval are represented by blue traces. White circles indicate the locations of the spacecraft at 10:03 UT.

21 min lag between the spacecraft measurements; it also showed that some of the large amplitude oscillations observed by Cluster around 10:30 UT (see Figure 1) were well correlated with solar wind fluctuations and thus were not magnetopause crossings.

[12] The simulation code solves the resistive one-fluid MHD equations as an initial value problem, using an explicit conservative predictor-corrector scheme for time stepping, and hybridized numerical fluxes for spatial finite differencing. A description of the code can be found elsewhere [*Raeder et al.*, 1995, 1996, 1997; *Berchem et al.*, 1995a, 1995b, 1998a, 1998b]. Two important features of that model are that an ionospheric submodel is used to calculate height-integrated Hall and Pedersen conductivities, and that the simulation model includes a resistive term in Ohm's law, $\mathbf{E} = -\mathbf{v} \times \mathbf{B} + \eta\,\mathbf{j}$. Resistivity ($\eta$) is a nonlinear function of the local current density $\mathbf{j}$, such that $\eta = \alpha j^2$, where α is an empirically determined parameter ($\alpha \ll 1$) [*Raeder et al.*, 1996]. Similar models have been used for local MHD simulations [e.g., *Sato and Hayashi*, 1979] and are based on the assumption that current-driven instabilities are responsible for the anomalous resistivity that produces reconnection. To avoid spurious dissipation we use a threshold δ, also empirically determined, that is a function of the local current density and magnetic field ($\eta = 0$ unless $|j|\Delta/(|B| + \varepsilon) \geq \delta$; Δ = local grid size; $\varepsilon \ll 1$). The resolution of the simulation grids used in the runs presented in this paper is about 0.15 R_E in the magnetopause subsolar region. However, because the resolution of the grid decreases with its distance to the Sun-Earth axis, grid sizes of about 0.3 R_E are common in regions where the magnetopause crosses the terminator.

[13] Figure 3 shows the superposition of the simulation data streams over a time series of the magnetic field measured at Cluster (Figure 3 (left)) and TC-1 (Figure 3 (right)). Comparison of the simulated data at the location of

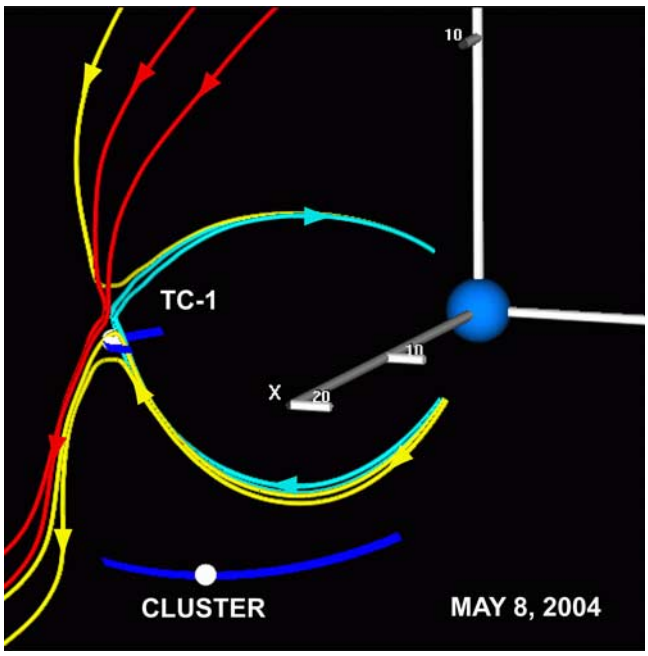

Figure 6. Close-up of the dawnside-merging region shown in Figure 5. Cluster and TC-1 trajectories during the 06:00–16:00 UT time interval are represented by blue traces. White circles indicate the locations of the spacecraft at 10:03 UT. Unconnected, open, and closed field lines are shown in red, yellow, and turquoise, respectively. Typical *X*-type reconnection geometry is readily apparent indicating the occurrence of magnetic reconnection.

the spacecraft (thick traces) with the spacecraft measurements indicates that the simulation is successfully reproducing the observations. The magnetopause crossings and trends in the magnetospheric field observed by Cluster are well reproduced by the simulation (Figure 3 (left)). As expected, the computational grid is not fine enough for the simulation to reproduce small-amplitude oscillations or the sharp gradients observed by the spacecraft as they cross the magnetopause. However, the global simulation does not track very well TC-1 measurements (Figure 3 (right)). Shifting the location of the virtual TC-1 spacecraft (shown by thick traces in Figure 4) toward dawn by 0.5 R_E significantly improves the agreement between the simulation results and the observations by capturing the incursions of the TC-1 spacecraft into the magnetosheath. Nonetheless, the simulation has difficulty in rendering quick reentries into the magnetospheric field, suggesting that the grid is too coarse in that region to resolve the full dynamics of the magnetopause.

[14] Results of the simulations have been used to follow the topology evolution of the magnetic field at the magnetopause as the IMF varies during the event [*Berchem et al.*, 2005, 2006]. This paper focuses on the specific time interval around 10:03 UT, during which the magnetic shear angle between the magnetosphere and the incoming solar wind was ~160°. At that time the Cluster spacecraft were in the magnetosheath whereas the TC-1 spacecraft was reentering the magnetosphere and crossing the magnetopause [x_{GSE} = 2.92; y_{GSE} = −12.84; z_{GSE} = −1.34 R_E] after a series of rapid incursions into the magnetosheath.

[15] Figure 5 is a composite picture of two- and three-dimensional renderings of the dayside magnetosphere obtained using the simulation. The snapshot reveals the topology of the merging region for the 10:03 UT magnetopause crossing viewed from 14:00 LT. The backdrop of the picture is a two-dimensional cross section (*Y-Z* plane) of the magnetotail taken at $x = -10$ R_E showing color contours of the plasma beta. The magnetotail lobes are readily associated with the regions of low-beta plasma (deep blue contours) separated by the high-beta plasma of the plasma sheet (red contours) and bounded by the magnetopause (transition between green and yellow contours). A three-dimensional isosurface of plasma beta (=100) complete the picture with the same color coding as that of the cross section contours. It delineates three regions of high beta. The forward-most region is bounded by the bow shock and corresponds to the region of the magnetosheath where most of the magnetic field lines connected to the Earth converge before crossing the bow shock. The two other regions of high-beta plasma are at the magnetopause near the equatorial plane and extend from the dawn and dusk flanks toward the dayside. A strong east-west asymmetry exists. The dawn region extends toward the dayside region, almost reaching the subsolar region, whereas the dusk region spans a much narrower region near the dusk flank. Magnetic field lines threading these two regions were traced, and open and closed field lines are shown in yellow and turquoise, respectively.

[16] The inset in Figure 5 shows magnetic field lines hidden by the isosurface in the dawn region. Cluster and TC-1 trajectories during the 06:00–16:00 UT time interval are represented by blue traces. White diamonds indicate the locations of the spacecraft at 10:03 UT. The picture reveals that open field lines make sharp kinks in the high-beta plasma regions, thereby indicating the occurrence of magnetic nulls and hence magnetic reconnection in the dawn and dusk regions. As a result the merging region is split into two regions, as predicted by the antiparallel-merging model, when the IMF is southward and has a finite B_y component [*Crooker*, 1979; *Luhmann et al.*, 1984]. However, the locations of the merging regions differ significantly from those of the model [*Crooker*, 1979] because of the presence of a significant B_x component in the IMF.

[17] A typical *X*-type reconnection geometry is readily apparent in a close-up of the dawnside-merging region shown in Figure 6. Unconnected magnetosheath field lines are shown in red. Figure 6 shows that the simulation predicts the occurrence of reconnection north of the TC-1 spacecraft. Such a topology is consistent with the fast plasma flows (V_z and V_y < 0) measured by the CIS and Peace experiments onboard TC-1 around 10:00 UT, as well as with the polarities of the numerous FTEs observed on that pass [*Marchaudon et al.*, 2005]. Figure 7 and its inset display the same region as in Figure 6, but as viewed from higher latitude and from noon, respectively. These views reveal the formation of a merging line that extends from about 7 to 10 MLT, or about 7 R_E in length. In addition, they clearly show that the 3-D geometry of the merging region

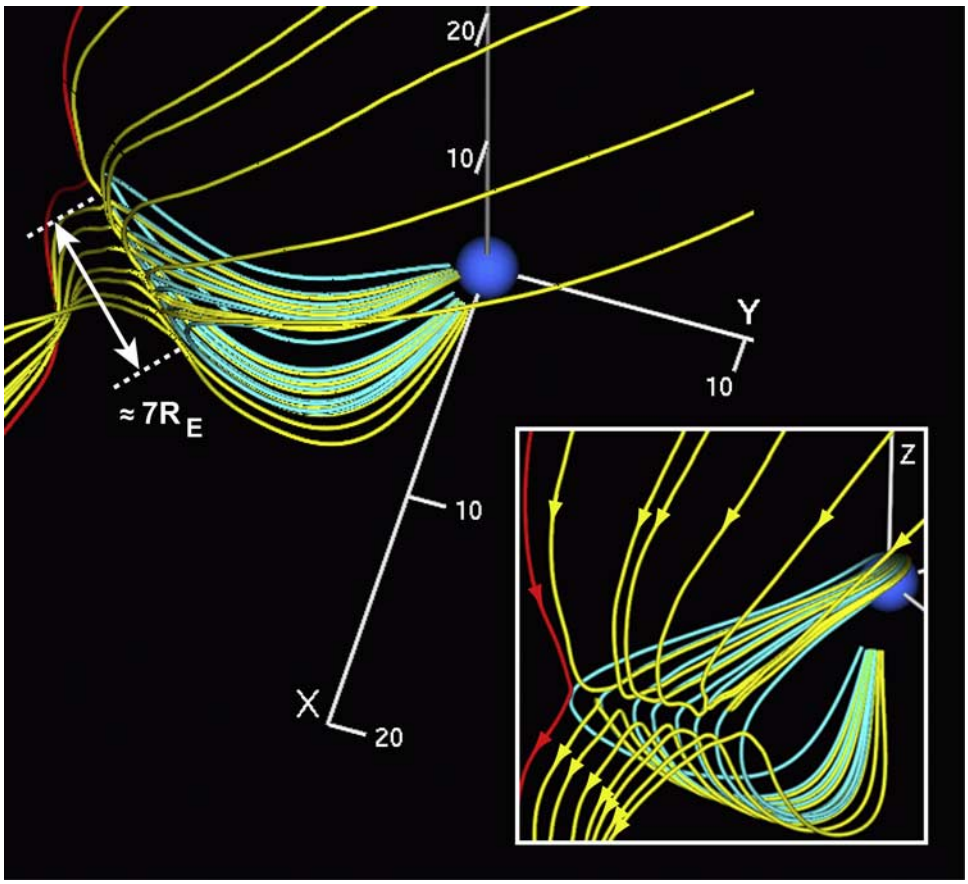

Figure 7. High-latitude view of the dawnside-merging region shown in Figure 6. Unconnected, open, and closed field lines are shown in red, yellow, and turquoise, respectively. The merging line region extends from about 7 to 10 MLT or about 7 R_E in length. The inset shows an extreme close-up of the dawnside-merging region viewed from 9:00 LT. It shows that the 3-D geometry of the merging region is made up of the radial juxtaposition of planes displaying *X*-type reconnection geometries.

made up of the radial juxtaposition of planes displaying *X*-type reconnection geometries.

3. The 6 April 2004 Event

[18] The second Cluster and TC-1 conjunction used in our study occurred on 6 April 2004. *Dunlop et al.* [2005] studied this event extensively. Two features make this conjunction particularly interesting for synoptic studies of the structure and dynamics of magnetic reconnection at the dayside magnetopause. First, during the event studied the Cluster spacecraft were exploring the high-latitude Northern Hemisphere, whereas TC-1 was in the Southern Hemisphere at mid latitudes. Second, the spacecraft were all on outbound passes and on the dawn side, with Cluster's orbit closer to the noon-midnight meridian than TC-1's. This orbital configuration and favorable timing provided a unique capability for the spacecraft to cross the magnetospheric boundary of both hemispheres in the same range of local time and almost simultaneously. Cluster crossed the magnetopause at 4:15 UT [x_{GSE} = 6.5; y_{GSE} = −1.0; z_{GSE} = 6.4 R_E] and TC-1 at 4:33 UT [x_{GSE} = 4.0; y_{GSE} = −8.9; z_{GSE} = −1.2 R_E]. Figure 8 shows magnetic field vectors measured by Cluster and TC-1 on 6 April 2004. The data are displayed in boundary-normal coordinates [e.g., *Russell and Elphic*, 1978]. Measurements from Cluster 3 (red traces) have been superimposed over TC-1 data (blue traces). Numerous flux transfer event (FTE) signatures can be identified in both spacecraft passes. *Dunlop et al.* [2005] analyzed these data in great detail. An important fact they noticed is that the FTE polarities (∓) observed by TC-1 were opposite those observed by Cluster (±), indicating that the FTEs were moving in opposite directions. The FTE polarities suggested that Cluster was located north of the reconnection site, whereas TC-1 was lying south of it. Furthermore TC-1 observed fewer FTEs than Cluster did, and those observed had smaller amplitudes, suggesting that they might have resulted from a weaker reconnection process [*Dunlop et al.*, 2005].

[19] Figure 9 shows ACE solar wind plasma parameters [*McComas et al.*, 1998] and magnetic field [*Smith et al.*, 1998] observations [x_{GSE} = 226.8; y_{GSE} = 37.4; z_{GSE} = −21.6 R_E]. It is clear that solar wind conditions were fairly steady prior to the conjunction event. The solar wind's ion density was about 6 cm^{-3} and its speed was of the order of 530 km/s, resulting in a dynamic pressure of about 3 nPa. The IMF was mostly southward, with a large $B_y < 0$ component during most of the event. Another noteworthy feature of the event is the large east-west component ($V_y \approx$ 120 km/s) of the solar wind velocity. Lagged plasma and

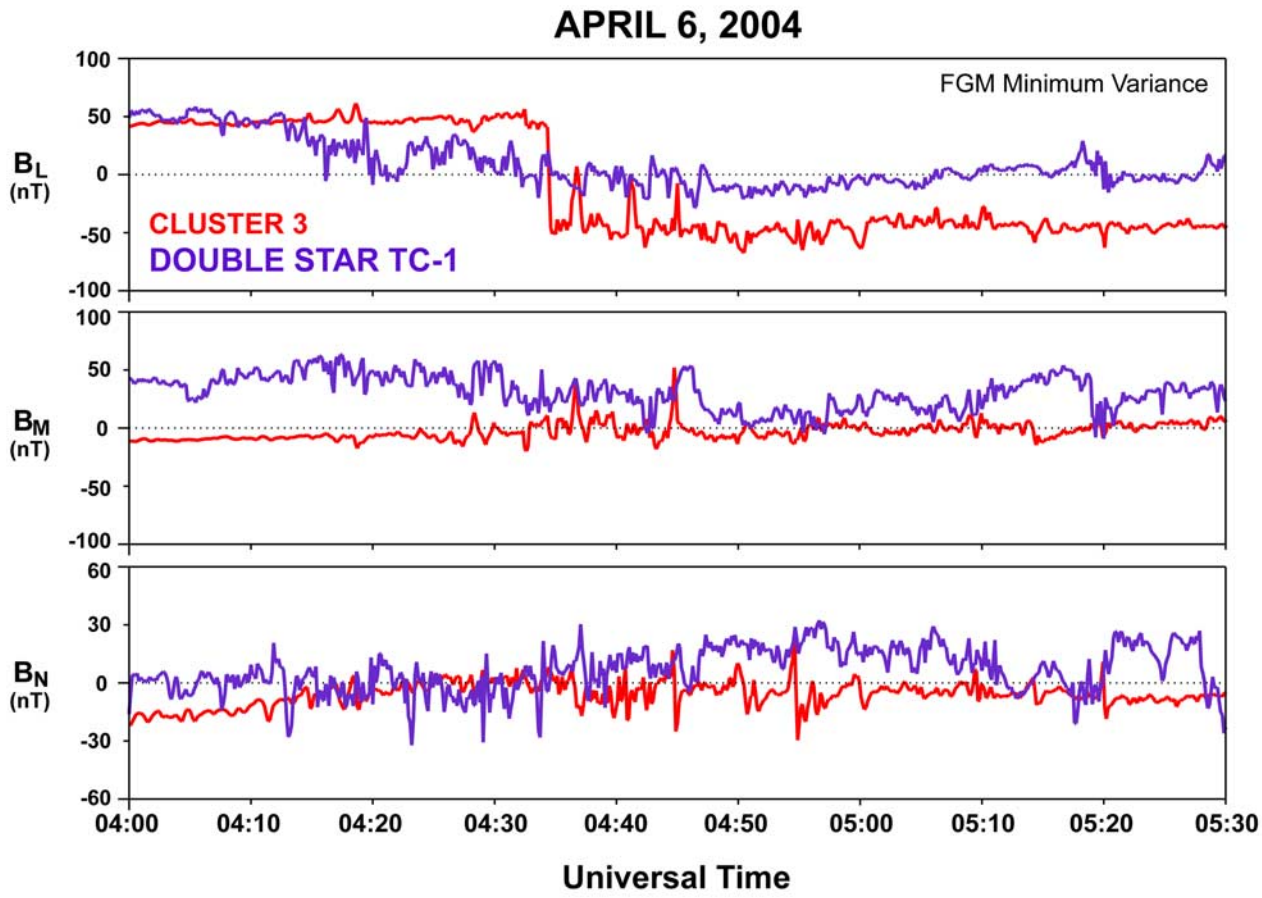

Figure 8. Magnetic field vectors measured by Cluster 3 (red) and TC-1 (blue) on 6 April 2004. The data are displayed in boundary-normal coordinates. Cluster and TC-1 crossed the magnetopause at 4:15 and 4:33 UT, respectively. Numerous FTE signatures can be identified in both traces; FTE polarities ($\mp$) observed by TC-1 were opposite those observed by Cluster ($\pm$), indicating that the FTEs were moving in opposite directions.

magnetic field measurements from the ACE spacecraft were used as input to a global MHD simulation (see brief description above). Figure 10 displays data streams from the simulations (thick traces) superimposed over the magnetic field measurements from the Cluster 3 (Figure 10 (left)) and TC-1 (Figure 10 (right)) spacecraft. Though the grid resolution is too coarse to reproduce the sharp gradients and FTEs observed by the spacecraft, the simulation is fairly successful at reproducing the trends of the magnetic field seen in the data.

[20] Results from the global simulation for the time when TC-1 crossed the magnetopause (04:33 UT) are shown in Figure 11. At that time the IMF, where it was interacting with the magnetopause, was almost horizontal ($B_z \approx 0$). The format used is similar to that used in Figure 5. The backdrop of the picture is a two-dimensional cross section (*Y-Z* plane) showing color contours of the plasma beta. The cut is taken at $x = -10\ R_E$ and viewed from 2:00 LT. The magnetotail lobes (deep blue contours) and plasma sheet (red contours) are evident. This is a close-up view; as a result only a fraction of the magnetospheric boundary (transition between green and yellow contours) is visible. A three-dimensional isosurface of plasma beta (=100) are superimposed over the two-dimensional cut. It has been rendered using the same color coding as that of the cross section contours and delineates several regions of high-beta plasma. The most distant regions (around $x = -10\ R_E$) are parts of the plasma sheet, whereas the closest ones are parts of the magnetopause. There is an additional region of high-beta plasma located on the closed field lines of the dusk flank. This region results from a constriction of the dusk flank region by the large transverse component of the solar wind velocity. In fact the global topology of the dusk flank is reminiscent of the central plasma sheet. Magnetic field lines have been traced from regions of high beta at the magnetopause. They indicate the occurrence of reconnection in the high-latitude dawn region of the cusp in the Northern Hemisphere and below the dusk equatorial flank in the Southern Hemisphere. The two merging regions found are fairly consistent with the antiparallel-merging model for clock angles of $\approx 90°$ [*Crooker*, 1979; *Luhmann et al.*, 1984].

[21] As we mentioned above, recent studies have shown the occurrence of component reconnection in global MHD simulation results [e.g., *Dorelli and Raeder*, 2005, *Dorelli et al.*, 2007; *Berchem et al.*, 2006]. Almost 20 years ago,

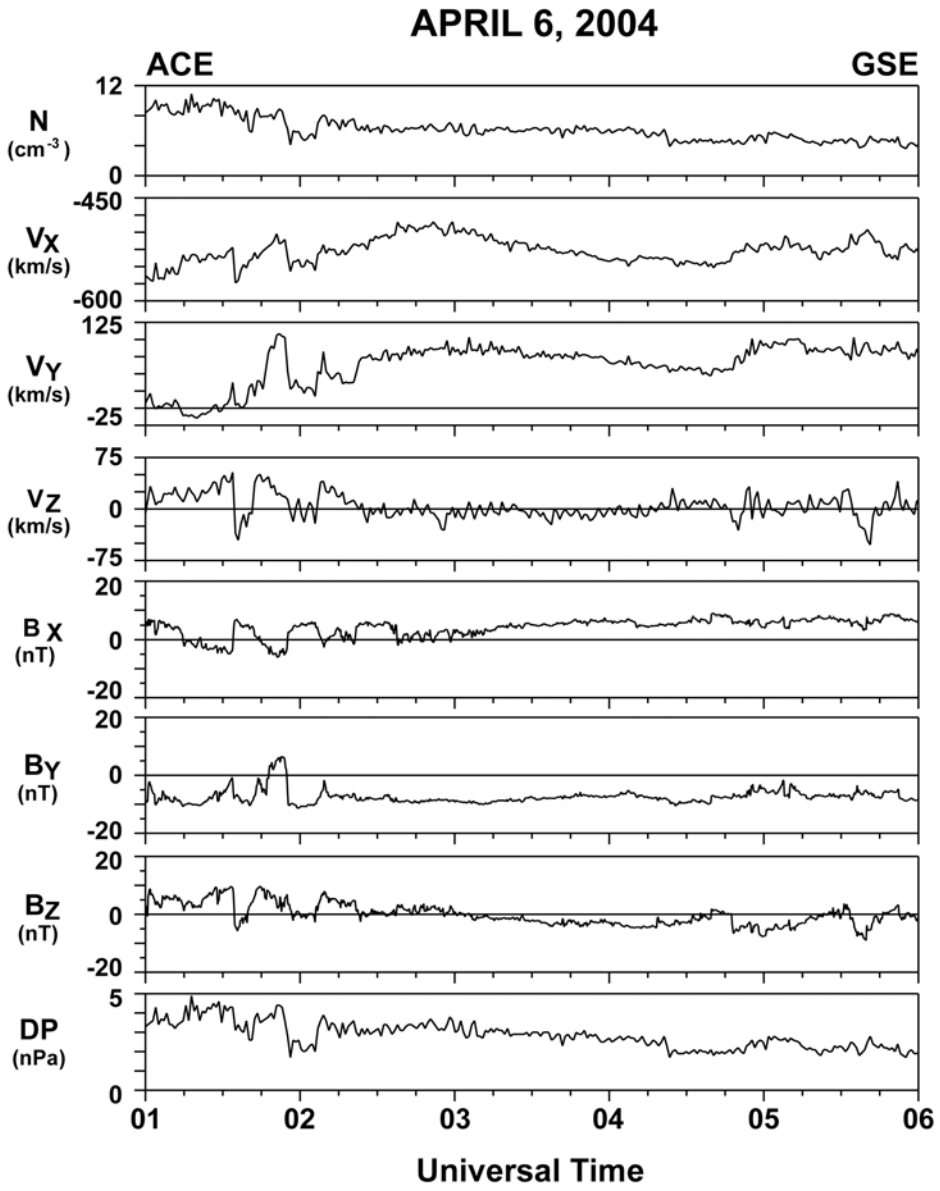

Figure 9. ACE solar wind plasma parameters and magnetic field observations displayed in GSE for 6 April 2004. There is a lag of about 50 min between ACE and Cluster measurements.

Schindler et al. [1988] and *Hesse and Schindler* [1988] pointed out that 3-D reconnection can occur in the absence of nulls and separatrices and suggested that the condition $\int E_{\|} ds \neq 0$, where $E_{\|}$ is the parallel electric field and the integral is taken along a particular magnetic field line (ds), was a necessary and sufficient condition for general magnetic reconnection. This requirement comes from the fact that the parallel component of the total electric field $\mathbf{E} = -\mathbf{v} \times \mathbf{B} + \eta\, \mathbf{j}$ vanishes except in regions of strong dissipation. However, as noted by *Priest and Forbes* [2000] such a condition is quite broad and includes many diffusive phenomena that are not exclusively associated with reconnection (e.g., double layers and shocks). When looking for reconnection regions in the simulation results, a powerful practical diagnostic is thus to compute the parallel electric field at the magnetopause. Tracing actual field lines can be then used to verify the successful identification of the merging region and to visualize the magnetic field topology of its near vicinity.

[22] Figure 12 shows a close-up of the subsolar magnetosphere at the time of the TC-1 crossing (04:33 UT). It is viewed from the same angle (14:00 LT) used in Figure 11. Two field lines are traced to show the 90° shear angle between the magnetospheric field (blue closed field line) and the IMF (red unconnected field line). The yellow bubble-like shapes displayed are three-dimensional renderings of the $E_{\|}$ = 0.5 mV/m isosurface. Tracing field lines threading these regions of high electric field shows that they are open (yellow field lines). The presence of such open field lines in that region indicates the occurrence of merging for a 90° shear angle between the local magnetosheath field and the geomagnetic field. This suggests that merging is occurring through component reconnection at the dayside magnetopause and, as we discuss below, that it is

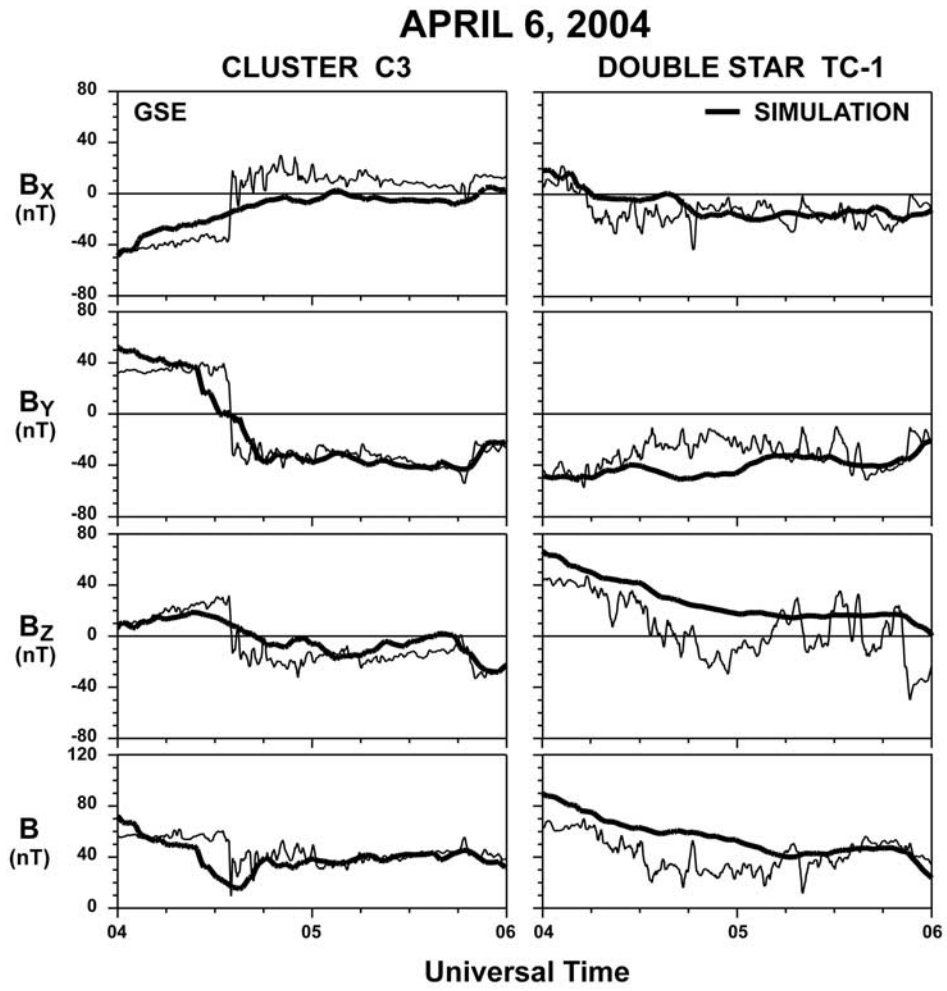

Figure 10. Data streams from the simulation (thick traces) superimposed over the magnetic field measurements from (left) Cluster 3 and (right) TC-1 for magnetopause crossings on 6 April 2004.

constrained to a limited region of the subsolar magnetopause. Together with the previous results, this analysis of the simulation reveals that component and antiparallel merging occur simultaneously at the dayside magnetopause.

[23] To conclude, we consider the observations to determine whether they support the simulation results. Figure 13 displays the large-scale topology of the dayside magnetopause predicted by the global MHD simulation of the event. This illustration shows the superposition of the two merging systems described in Figures 11 and 12. The merging occurring in the dusk flank is omitted to simplify the picture. Field lines are viewed from 11:00 LT, and the same color coding is used: red, yellow and turquoise indicate unconnected, open, and closed field lines, respectively. The green ribbons represent the trajectories of the Cluster and TC-1 spacecraft. Tracing field lines passing by TC-1's location suggests that TC-1 was most likely located in a region threaded by southern field lines that were moving dawnward after being opened by component reconnection at low latitudes. However, Cluster appears to be located at too high a latitude to observe the matching northern field lines that were also opened in the subsolar region before moving toward dusk. In fact, the simulation indicates that the open field lines observed by Cluster were most likely formed at high latitudes through antiparallel reconnection. It is readily seen that the locations of both merging regions and the motion of the tubes are consistent with the different FTE polarities observed by each spacecraft. Furthermore, the fact that Cluster appears to be closer to the high-latitude reconnection region also seems consistent with Cluster's observing stronger reconnection signatures than TC-1 does. The invocation of antiparallel merging to explain Cluster observations differs somewhat from the conclusions of *Dunlop et al.* [2005]. Their interpretation of the event is based on *Cooling et al.*'s [2001] model, which suggested that both sets of FTEs were related to the formation of a single tilted merging line in the subsolar magnetopause.

4. Discussion

[24] Results from the studies presented in the two previous sections provide noteworthy information about the large-scale configuration of magnetic reconnection at the magnetopause. Results from the global simulation for the 8 May event clearly show the occurrence of antiparallel merging at the low-latitude dayside magnetopause. Some interesting features of the merging are evident in Figures 5 and 7. First, while reconnecting field lines far from the reconnection

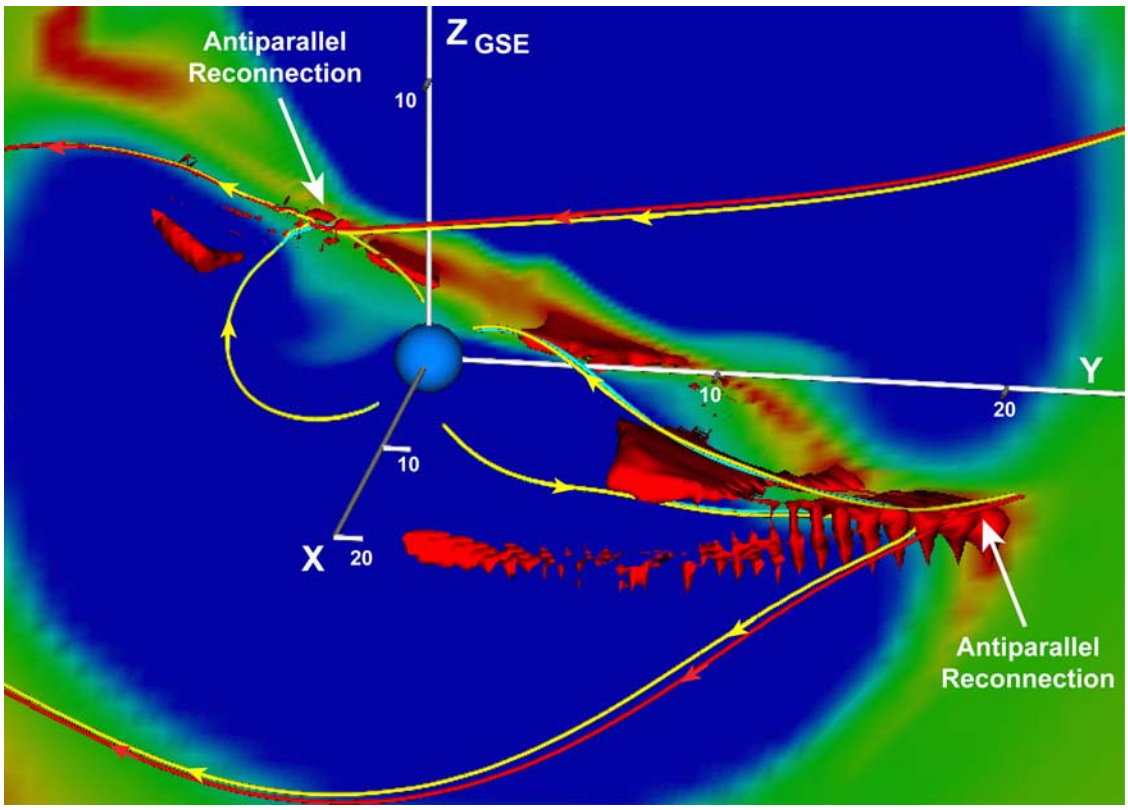

Figure 11. Composite picture of two- and three-dimensional renderings of the dayside magnetosphere obtained using the simulation of the 4:33 UT magnetopause crossing on 6 April 2004. The dayside magnetopause is viewed from 14:00 LT. The backdrop of the picture is a two-dimensional cross section (*Y-Z* plane) of the magnetotail taken at $x = -10\ R_E$ showing color contours of the plasma beta. A three-dimensional isosurface of plasma beta (=100) completes the picture with the same color coding as that of the cross-section contours. Unconnected, open, and closed field lines are shown in red, yellow, and turquoise, respectively. They indicate the occurrence of reconnection in the high-latitude dawn region of the cusp in the Northern Hemisphere and below the dusk equatorial flank in the Southern Hemisphere. The two merging regions found are fairly consistent with the antiparallel-merging model for clock angles of $\approx 90^\circ$.

region have a relatively strong B_y component consistent with the IMF orientation, the field line segments near the reconnection region have a much weaker B_y component. As a result, the draped magnetosheath aligns with the geomagnetic field at a much lower latitude than expected and produces a merging topology that very much resembles the two-dimensional geometry expected for more southward IMF conditions. This suggests that the geometry of the interaction is much more complicated than topology expected from simple vector addition of the magnetosheath and the geomagnetic field. More work is needed to determine whether this apparent minimization of the magnetic shear in the reconnection region is connected to the draping of the magnetosheath field over the magnetopause or is instead a separate physical process.

[25] A second unexpected and related feature predicted by the simulation of the 8 May event is the location of the main reconnection region. While the magnetic field topology found is reminiscent of subsolar reconnection for southward IMF, the reconnection region is unexpectedly offset toward dawn (e.g., Figure 7). Tracing isosurfaces of the parallel electric field indicates that component merging is also occurring, but is concentrated in the morning sector. Our current analysis of the simulation results does not indicate the occurrence of reconnection in the afternoon sector, and thus we do not find a continuous region of merging (reconnection separator) between the dawn and dusk regions of antiparallel merging as predicted by three-dimensional reconnection theory. The strong reconnection signatures observed by TC-1 confirms the simulation's prediction that merging occurs in the dawn sector. However, because of the absence of simultaneous measurements in the subsolar region and dusk sector, we cannot assess the prediction of the simulation regarding the confinement of the merging region to the dawn and morning sectors. A minimum variance analysis of the solar wind magnetic field reveals that the normal of the large-scale discontinuities embedded in the IMF is $\mathbf{n} = 0.633, 0.005, 0.770$, and hence the direction of the normal makes a wide angle with the Sun-Earth axis. As a result, the first interaction of the IMF discontinuities with the magnetopause occurs away from the subsolar region. The combination of that effect together with the large B_y component might cause the asymmetry of the merging regions. More systematic studies are required to

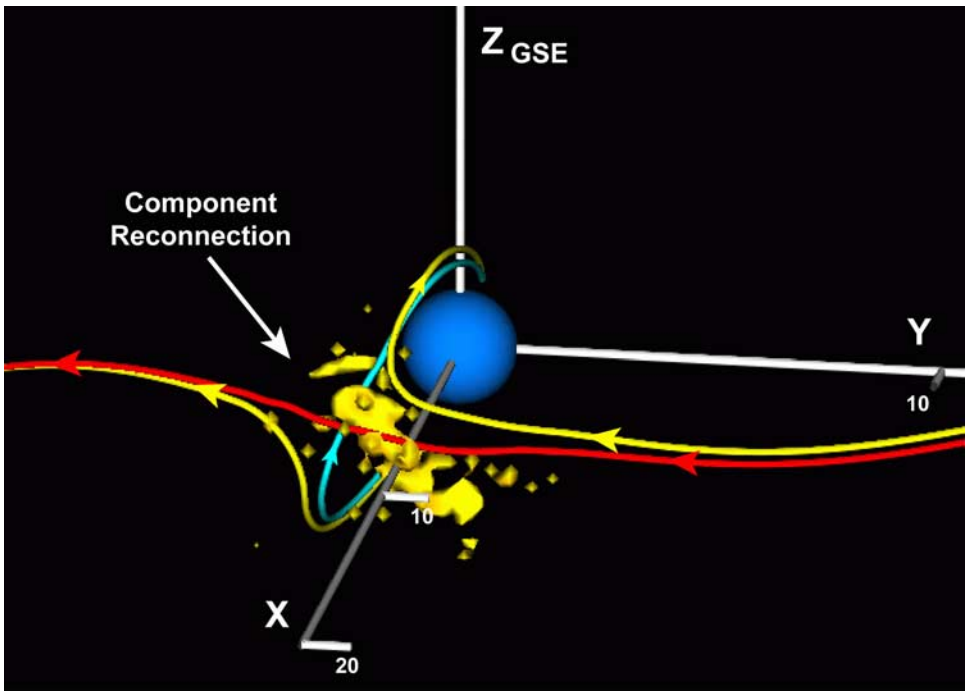

Figure 12. Close-up of the subsolar magnetosphere at the time of the TC-1 crossing (04:33 UT) on 6 April 2004. It is viewed from 14:00 LT. Two field lines are traced to show the 90° shear angle between the magnetospheric field (blue closed field line) and the IMF (red unconnected field line). The yellow bubble-like shapes displayed are three-dimensional renderings of the $E_{||}$ = 0.5 mV/m isosurface. The presence of open field lines (yellow) indicates the occurrence of component merging at the subsolar magnetopause.

determine whether the incidence angle of large-scale discontinuities with the dayside magnetopause is an important factor in determining where reconnection occurs.

[26] Simulation results for the 6 April event appear to be more conventional, though the large east-west component ($V_y \approx 120$ km/s) of the solar wind velocity produces a strong asymmetry in the locations where antiparallel merging occurs. The most interesting feature is the prediction of the simultaneous occurrence of component and antiparallel merging by the global MHD simulation and its consistency with Cluster and TC-1 observations. This is an important result since it indicates that the two processes are not mutually exclusive, and thus determining whether merging at the dayside magnetopause occurs through component or antiparallel reconnection is no longer the issue. However, the evidence of the coexistence of component or antiparallel reconnection prompts numerous new and fundamental questions about the actual nature of the large-scale topology of merging at the dayside magnetopause, and in particular makes establishing the topology of the merging region of some importance. Although tracing field lines confirms the occurrence of reconnection in the subsolar region in the global simulation, it is debatable whether the component-merging region is patchy and limited to the subsolar region, as the 3-D isosurface of strong $E_{||}$ (shown in yellow on Figure 12) suggest. The three-dimensional model of magnetic reconnection [e.g., *Greene*, 1988; *Siscoe et al.*, 2001; *Dorelli et al.*, 2007] predicts that reconnection forms a continuous region of merging that connects the two regions of antiparallel merging (magnetic nulls). It is clear that the isosurface of $E_{||}$ = 0.5 mV/m used in our study visualizes only the regions where the field is strong. Weaker parallel electric fields are found in the region separating open field lines between both hemispheres. This is consistent with previous simulation studies that found the parallel electric field was distributed along the topological separator line. For example, *Siscoe et al.* [2001] found that the reconnection voltage in a global MHD simulation for duskward IMF was weaker at the null points than at the subsolar point by about a factor three.

[27] The relative spatial limitation of component merging to the subsolar region indicated by the isosurface of the parallel electric field is also apparent when searching for accelerated flows away from the subsolar region. The high-speed flows indicated by isosurfaces of the V_z component (±115 km/s) of the bulk velocity in Figure 14 appear to be concentrated in the subsolar region of the magnetopause. These results are not inconsistent with the concept of a topological reconnection separator predicted by theory of three-dimensional reconnection. Nevertheless, one can question whether the entire separator region is active or only a portion of it exhibits the classical signatures of reconnection. This concern is of even more consequence when considering northward IMF cases, for which the theory predicts that the reconnection separator crosses over the subsolar region [e.g., *Dorelli et al.*, 2007]. To resolve this issue we need both to refine the diagnosis of 3-D reconnection in the global simulations and to predict clear signatures of a reconnection separator that can be identified in observations.

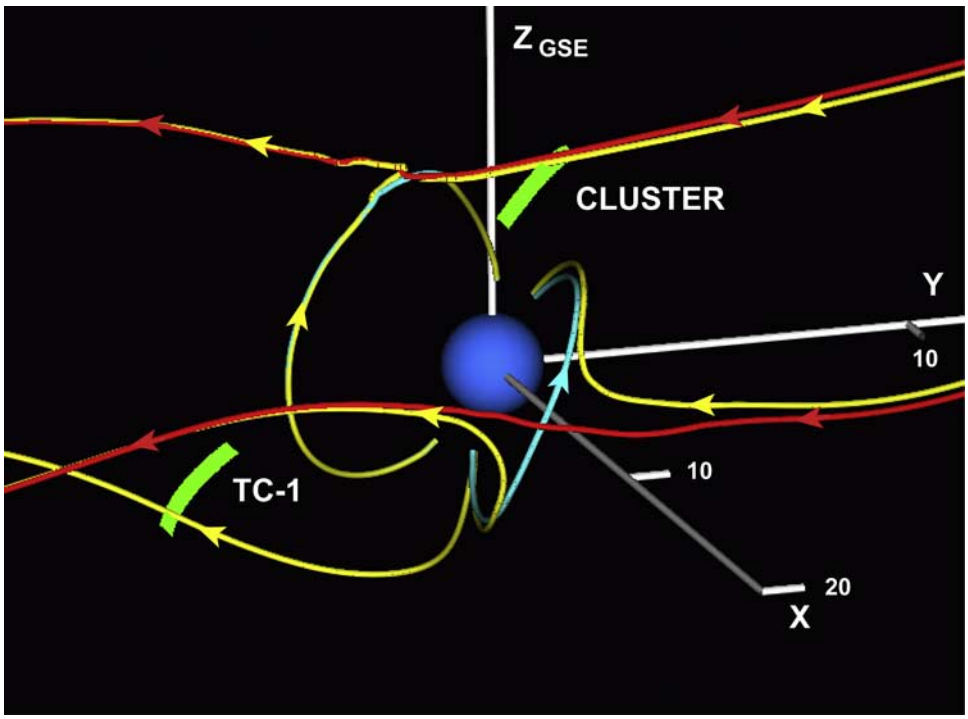

Figure 13. Display of the large-scale topology of the dayside magnetopause predicted by the global MHD simulation of the 6 April 2004 event. Merging occurring in the dusk flank is omitted to simplify the picture. Field lines are viewed from 11:00 LT. Red, yellow, and turquoise indicate unconnected, open, and closed field lines, respectively. The green ribbons represent the trajectories of the Cluster and TC-1 spacecraft. The open field line passing by TC-1's location suggests that TC-1 was most likely located in a region threaded by southern field lines that were moving dawnward after being opened by component reconnection at low latitudes. Cluster appears to be located at too high a latitude to observe the matching northern field lines that were also opened in the subsolar region before moving toward dusk. The simulation indicates that the open field lines observed by Cluster were most likely formed at high latitudes through antiparallel reconnection.

[28] Another set of issues is related to the effects inherent to the model, such as resistivity, either explicit (resistive term in Ohm's law) or numerical (e.g., grid resolution at high latitudes). Figure 15 shows results from several global MHD simulation runs that were carried out for the different values of the resistivity coefficient α ($\eta = \alpha j^2$) and threshold δ used in the resistivity model. All simulations show the simultaneous occurrence of component and antiparallel merging. However, they indicate that the merging region, as identified by green isosurfaces of strong $E_{\|}$, grows with increasing resistivity values and becomes patchy when a resistivity threshold ($\delta \neq 0$) is used in the model. The axes of the regions found are aligned along a direction similar to the tilted merging line predicted by component merging models. Figure 15 (middle) shows that for a high-resistivity (and somewhat unrealistic) coefficient ($\alpha = 1$), the region of component merging predicted by the simulation extends toward latitudes higher than those found for the lower-resistivity cases. When comparing the directions of the axis of merging regions found in the 3 cases, it is interesting to note that the main axis of the high-resistivity case has a greater tilt ($\approx 10^\circ$ counterclockwise) than the other two cases have. Of course the effects of other parameters, such as grid size in the high-latitude region, also need to be investigated to gain a better assessment of the dependence of the simulation results on the model parameters. Nevertheless, these initial results illustrate the complexity of predicting merging topology using global models and the necessity of comparing their predictions with multiple spacecraft observations. In particular, from the results shown above it appears that determining the extent and tilt of the merging region could help constrain some of the models' parameters.

5. Summary

[29] Most previous investigations of the merging region's large-scale properties have been hampered by the lack of simultaneous local measurements at the dayside magnetopause having the necessary spatial coverage. Conjunction events between Cluster and TC-1 provide a unique opportunity to investigate the large-scale configuration of magnetic reconnection at the dayside magnetopause. In particular such conjunction events are invaluable for testing the accuracy of global models. In this paper we examined two events that involve southward IMF with significant transverse components (B_y). The first events occurred on 8 May 2004 while both spacecraft were exploring the dawn flank of the magnetosphere. TC-1 was skimming the equatorial magnetopause while Cluster explored higher latitudes. Results from a global simulation of the event

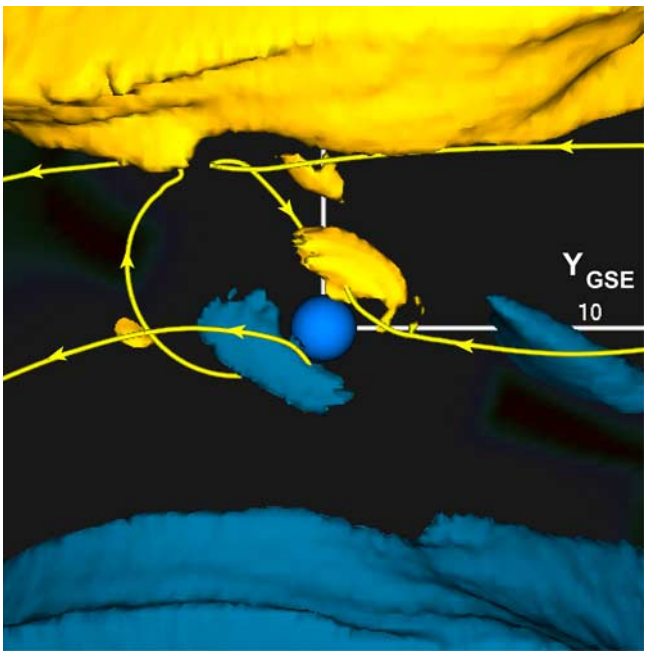

Figure 14. Rendering of the dayside magnetosphere viewed from Sun, showing the isosurfaces of the V_z component of the bulk velocity for +115 km/s (yellow) and −115 km/s (blue) for 6 April 2004 event. In addition to the large-scale northward and southward flows in the magnetosheath occurring at high latitudes, the isosurfaces reveal the presence of high-speed flows in the subsolar region that are consistent with the occurrence of component merging in that region.

revealed the formation of a near-equatorial merging line of about 7 R_E in the morning sector, and that the three-dimensional geometry of the merging region was mostly a radial juxtaposition of planes displaying *X*-type reconnection geometries. The second conjunction event was on 6 April 2004. During this event, Cluster was located at high latitudes and close to the noon-midnight meridian while TC-1 was exploring the dawnside at low latitudes. Analysis of the simulation results using isosurfaces of plasma beta and the parallel electric field revealed unambiguously that both antiparallel and component merging occurred simultaneously during the event. The locations of the antiparallel merging sites, though distorted because of the draping of the field and the large transverse component of the solar wind velocity during the event, were for the most part consistent with merging patterns predicted by the antiparallel merging model. Plotting the parallel electric field indicated the component merging began in the subsolar magnetopause region. Simulation runs carried out for different parameters of the model indicate that the spread of the merging region depends on the local resistivity. The component-merging region, as determined by isosurfaces of strong values of the parallel electric field, grows with increasing resistivity values and becomes patchy when a resistivity threshold is used in the model. Although parallel electric fields are present in the region separating open field lines between the two hemispheres, our analysis of high-speed flows indicates that the region of component merging remains spatially constrained to the subsolar region where stronger parallel electric fields occur. These results definitely indicate a need for more systematic studies of 3-D reconnection, and particularly the necessity to establish

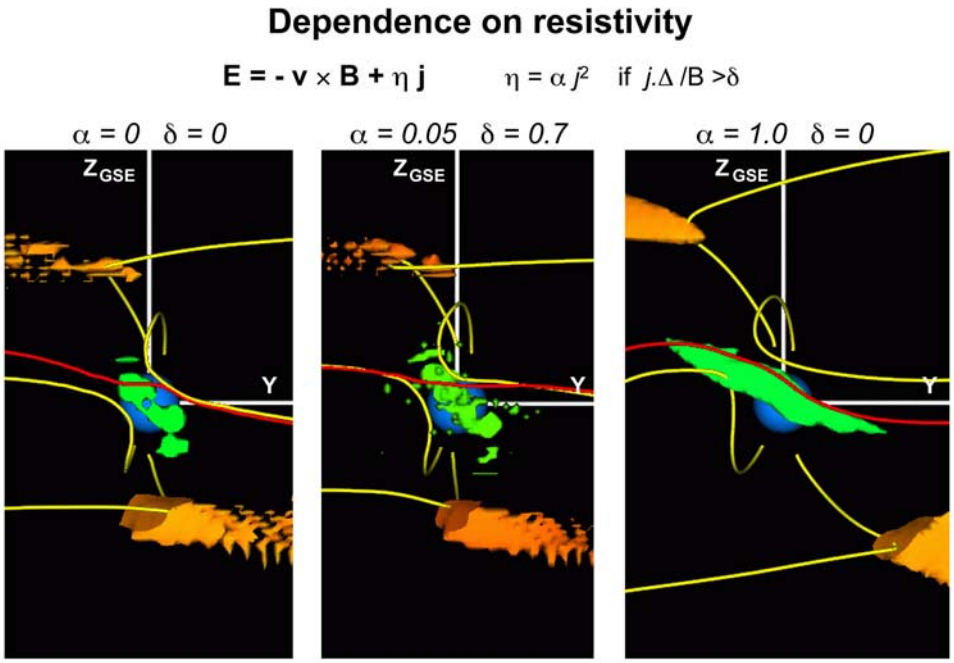

Figure 15. Results from three global MHD simulation runs that were carried out using the same solar wind input but for three different sets of the resistivity coefficient α ($\eta = \alpha j^2$) and threshold δ used in the resistivity model. Results for (left) ($\alpha = 0$, $\delta = 0$), (middle) ($\alpha = 0.05$, $\delta = 0.7$), and (right) ($\alpha = 1.0$, $\delta = 0$). The merging region, as indicated by green isosurfaces of strong $E_{||}$, grows with increasing resistivity values and becomes patchy when a resistivity threshold ($\delta \neq 0$) is used in the model.

clear observable spacecraft signatures that can be used to test the results of global models.

[30] **Acknowledgments.** Wind magnetic field and plasma measurements in the solar wind were kindly supplied by K. Ogilvie and R. Lepping (Goddard Space Flight Center, NASA). We thank D. McComas (Southwest Research Institute) and N. Ness (Bartol Research Institute, University of Delaware) for providing measurements from ACE's SWEPAM and MAG instruments, respectively. Computations were performed at the NASA Columbia Supercomputer Center. Research at UCLA was supported by NASA grants NNX07AG62G, NN05GK91G, and NNG05GG58G and NSF grant ATM-0603222.

[31] Amitava Bhattacharjee thanks the reviewers for their assistance in evaluating this manuscript.

References

Balogh, A., et al. (2001), The Cluster magnetic field investigation: Overview of in-flight performance and initial results, *Ann. Geophys.*, *19*, 1207.

Berchem, J. (2002), Comparison between global MHD simulation and CLUSTER observations, paper presented at XXVII General Assembly, Eur. Geophys. Soc., Nice, France, 21–26 April 2002.

Berchem, J., and C. T. Russell (1984), Flux transfer events on the magnetopause: Spatial distribution and controlling factors, *J. Geophys. Res.*, *89*, 6689, doi:10.1029/JA089iA08p06689.

Berchem, J., J. Raeder, and M. Ashour-Abdalla (1995a), Reconnection at the magnetospheric boundary: Results from global magnetohydrodynamic boundary, in *Physics of the Magnetopause, Geophys. Monogr. Ser.*, vol. 90, edited by B. U. Ö. Sonnerup, P. Song, and M. F. Thomsen, pp. 205–213, AGU, Washington, D.C.

Berchem, J., J. Raeder, and M. Ashour-Abdalla (1995b), Flux ropes at the magnetospheric boundary, *Geophys. Res. Lett.*, *22*, 1189, doi:10.1029/95GL01014.

Berchem, J., et al. (1998a), The distant tail at 200 R_E: Comparison between Geotail observations and the results of a global simulation, *J. Geophys. Res.*, *103*, 9121, doi:10.1029/97JA02926.

Berchem, J., et al. (1998b), Large-scale dynamics of the magnetospheric boundary: Comparison between global MHD simulation results and ISTP observations, in *Geospace Mass and Energy Flow: Results From the International Solar-Terrestrial Physics Program*, *Geophys. Monogr. Ser.*, vol. 104, edited by J. L. Horwitz, D. L. Gallagher, and W. K. Peterson, pp. 247–260, AGU, Washington, D. C.

Berchem, J., et al. (2005), Using Double Star and Cluster synoptic observations to test global MHD simulations of the large-scale topology of the dayside merging region, *Eos Trans. AGU*, *85*(47), Fall Meet. Suppl., Abstract SM23C-06.

Berchem, J., M. Dunlop, C. P. Escoubet, J. M. Bosqued, F. Pitout, Z. Pu, H. Reme, A. Balogh, and C. Carr (2006), Large-scale topology of dayside merging: Comparison of Global MHD Simulation results with measurements from the Double Star and Cluster spacecraft, paper presented at Eur. Geophys. Union Meet., Vienna, Austria, 10–14 April 2006.

Carr, C., et al. (2005), The Double Star magnetic field investigation: Instrument design, performance and highlights of the first year's observations, *Ann. Geophys.*, *23*, 2713.

Chandler, M. O., S. A. Fuselier, M. Lockwood, and T. E. Moore (1999), Evidence for component merging equatorward of the cusp, *J. Geophys. Res.*, *104*, 22,623, doi:10.1029/1999JA900175.

Cooling, B. M. A., C. J. Owen, and S. J. Schwartz (2001), The role of the magnetosheath flow in determining the motion of open flux tubes, *J. Geophys. Res.*, *106*, 18763, doi:10.1029/2000JA000455.

Cowley, S. W. H. (1973), A quantitative study of the reconnection between the Earth's magnetic field and the interplanetary field of arbitrary orientation, *Radio Sci.*, *8*, 903, doi:10.1029/RS008i011p00903.

Cowley, S. W. H. (1974a), On the possibility of magnetic fields and fluid flows parallel to the X-line in a re-connexion geometry, *J. Plasma Phys.*, *12*, 319.

Cowley, S. W. H. (1974b), Convection-region solutions for the re-connexion of antiparallel magnetic fields of unequal magnitude in an incompressible plasma, *J. Plasma Phys.*, *12*, 341.

Cowley, S. W. H. (1976), Comment on the merging of non-antiparallel magnetic field, *J. Geophys. Res.*, *81*, 3455.

Cowley, S. W. H., and C. J. Owen (1989), A simple illustrative model of open fluxtube motion over the dayside magnetopause, *Planet. Space Sci.*, *37*, 1461, doi:10.1016/0032-0633(89)90116-5.

Crooker, N. (1979), Dayside merging and cusp geometry, *J. Geophys. Res.*, *84*, 951, doi:10.1029/JA084iA03p00951.

Crooker, N., J. G. Lyon, and J. A. Fedder (1998), MHD model merging with IMF B_y: Lobe cells, sunward polar cap convection, and overdraped lobes, *J. Geophys. Res.*, *103*, 9143, doi:10.1029/97JA03393.

Dorelli, J. C., and J. Raeder (2005), On the IMF clock angle dependence of the dayside magnetopause reconnection rate, *Eos Trans. AGU*, *85*(47), Fall Meet. Suppl., Abstract SM12A-04.

Dorelli, J. C., M. Hesse, M. Kuznetsova, L. Rastaetter, and J. Reader (2004), A new look at driven magnetic reconnection at the terrestrial subsolar magnetopause, *J. Geophys. Res.*, *109*, A12216, doi:10.1029/2004JA010458.

Dorelli, J. C., A. Bhattacharjee, and J. Raeder (2007), Separator reconnection at Earth's dayside magnetopause under generic northward interplanetary magnetic field conditions, *J. Geophys. Res.*, *112*, A02202, doi:10.1029/2006JA011877.

Dunlop, M. W., et al. (2005), Coordinated Cluster/Double Star observations of dayside reconnection signatures, *Ann. Geophys.*, *23*, 2867.

Escoubet, C. P., M. Fehringer, and M. Goldstein (2001), The Cluster mission, *Ann. Geophys.*, *19*, 1197.

Fedder, J. A., J. G. Lyon, S. P. Slinker, and C. M. Mobarry (1995), Topological structure of the magnetotail as a function of interplanetary magnetic field direction, *J. Geophys. Res.*, *100*, 3613, doi:10.1029/94JA02577.

Fuselier, S. A., B. L. Anderson, and T. G. Onsager (1997), Electron and ion signatures of field line topology at the low-shear magnetopause, *J. Geophys. Res.*, *102*, 4847, doi:10.1029/96JA03635.

Fuselier, S. A., K. J. Trattner, and S. M. Petrinec (2000a), Cusp observations of high- and low-latitude reconnection for northward IMF, *J. Geophys. Res.*, *105*, 253, doi:10.1029/1999JA900422.

Fuselier, S. A., S. M. Petrinec, and K. J. Trattner (2000b), Stability of the high-latitude reconnection site for steady northward IMF, *Geophys. Res. Lett.*, *27*, 473, doi:10.1029/1999GL003706.

Fuselier, S. A., H. U. Frey, K. J. Trattner, S. B. Mende, and J. L. Burch (2002a), Cusp aurora dependence on IMF Bz, *J. Geophys. Res.*, *107*(A7), 1111, doi:10.1029/2001JA900165.

Fuselier, S. A., J. Berchem, K. J. Trattner, and R. Friedel (2002b), Tracing ions in the cusp and low-latitude boundary layer using multispacecraft observations and a global MHD simulation, *J. Geophys. Res.*, *107*(A9), 1226, doi:10.1029/2001JA000130.

Gonzalez, W. D., and F. S. Mozer (1974), A quantitative model for the potential resulting from reconnection with an arbitrary interplanetary magnetic field, *J. Geophys. Res.*, *79*, 4186, doi:10.1029/JA079i028p04186.

Gosling, J. T., M. F. Thomsen, S. J. Bame, R. C. Elphic, and C. T. Russell (1990), Plasma flow reversals at the dayside magnetopause and the origin of the asymmetric polar cap convection, *J. Geophys. Res.*, *95*, 8073, doi:10.1029/JA095iA06p08073.

Greene, J. (1988), Geometric properties of three-dimensional reconnecting fields with magnetic nulls, *J. Geophys. Res.*, *93*, 8583, doi:10.1029/JA093iA08p08583.

Hesse, M., and K. Schindler (1988), A theoretical foundation of general magnetic reconnection, *J. Geophys. Res.*, *93*, 5559, doi:10.1029/JA093iA06p05559.

Hill, T. W. (1975), Magnetic merging in a collisionless plasma, *J. Geophys. Res.*, *80*, 4689, doi:10.1029/JA080i034p04689.

Kessel, R. L., S.-H. Chen, J. L. Green, S. F. Fung, S. A. Boardsen, L. C. Tan, T. E. Eastman, J. D. Craven, and L. A. Frank (1996), Evidence of high-latitude reconnection during northward IMF: Hawkeye observations, *Geophys. Res. Lett.*, *23*, 583, doi:10.1029/95GL03083.

Lepping, R. P., et al. (1995), The Wind magnetic field investigation, *Space Sci. Rev.*, *71*, 207, doi:10.1007/BF00751330.

Liu, Z.-X., et al. (2005), The Double Star mission, *Ann. Geophys.*, *23*, 2707.

Luhmann, J. G., R. J. Walker, C. T. Russell, N. U. Crooker, J. R. Spreiter, and S. S. Stahara (1984), Patterns of potential magnetic field merging sites on the dayside magnetopause, *J. Geophys. Res.*, *89*, 1739, doi:10.1029/JA089iA03p01739.

Marchaudon, A., et al. (2005), Simultaneous Double Star and Cluster FTEs observations on the dawnside flank of the magnetosphere, *Ann. Geophys.*, *23*, 2877.

Maynard, N. C., et al. (2001), Observation of the magnetospheric "sash" and its implications relative to solar-wind/magnetospheric coupling: A multisatellite event analysis, *J. Geophys. Res.*, *106*(A4), doi:10.1029/2000JA003004.

McComas, D. J., S. J. Blame, P. Barker, W. C. Feldman, J. L. Phillips, P. Riley, and J. W. Griffee (1998), Solar Wind Electron Proton Alpha Monitor (SWEPAM) for the Advanced Composition Explorer, *Space Sci. Rev.*, *86*, 563, doi:10.1023/A:1005040232597.

Moore, T. E., M.-C. Fok, and M. O. Chandler (2002), The dayside reconnection X line, *J. Geophys. Res.*, *107*(A10), 1332, doi:10.1029/2002JA009381.

Ogilvie, K. W., et al. (1995), SWE: A comprehensive instrument for the Wind spacecraft, *Space Sci. Rev.*, *71*, 55, doi:10.1007/BF00751326.

Onsager, T. G., and S. A. Fuselier (1994), The location of the magnetopause reconnection for northward and southward interplanetary magnetic field,

in *Solar System Plasmas in Space and Time*, *Geophys. Monogr. Ser.*, vol. 84, edited by J. L. Burch and J. H. Waite Jr., pp. 183–197, AGU, Washington, D. C.

Paschmann, G., I. Papamastorakis, W. Baumjohann, N. Sckopke, C. W. Carlson, B. U. Ö. Sonnerup, and H. Lühr (1986), The magnetopause for large magnetic shear: AMPTE/IRM observations, *J. Geophys. Res.*, *91*, 11,099, doi:10.1029/JA091iA10p11099.

Phan, T.-D., G. Paschmann, and B. U. Ö. Sonnerup (1996), Low-latitude dayside magnetopause and boundary layer for high magnetic shear: 2. Occurrence of magnetic reconnection, *J. Geophys. Res.*, *101*, 7817, doi:10.1029/95JA03751.

Priest, E., and T. Forbes (Eds.) (2000), Reconnection in three dimensions, in *Magnetic Reconnection: MHD Theory and Applications*, pp. 230–289, Cambridge Univ. Press, New York.

Raeder, J., R. J. Walker, and M. Ashour-Abdalla (1995), The structure of the distant geomagnetic tail during long periods of northward IMF, *Geophys. Res. Lett.*, 22, 349, doi:10.1029/94GL03380.

Raeder, J., J. Berchem, and M. Ashour-Abdalla (1996), The importance of small scale processes in global MHD simulations: Some numerical experiments, in *Physics of Space Plasmas*, edited by T. Chang and J. R. Jasperse, pp. 403–414, Mass. Inst. of Technol., Cambridge, Mass.

Raeder, J., et al. (1997), Boundary layer formation in the magnetotail: Geotail observations and comparisons with a global MHD simulation, *Geophys. Res. Lett.*, *24*, 951, doi:10.1029/97GL00218.

Russell, C. T., and R. C. Elphic (1978), Initial ISEE magnetometer results: Magnetopause observations, *Space Sci. Rev.*, *22*, 681, doi:10.1007/BF00212619.

Russell, C. T., J. A. Fedder, S. P. Slinker, X.-W. Zhou, G. Le, J. G. Luhmann, F. R. Fenrich, M. O. Chandler, T. E. Moore, and S. A. Fuselier (1998), Entry of the POLAR spacecraft into the polar cusp under northward IMF conditions, *Geophys. Res. Lett.*, *25*, 3015, doi:10.1029/98GL00355.

Sato, T., and T. Hayashi (1979), Externally driven magnetic reconnection and a powerful magnetic energy converter, *Phys. Fluids*, *22*, 1189, doi:10.1063/1.862721.

Sato, T., T. Shimada, M. Tanaka, T. Hayashi, and K. Watanabe (1986), Formation of field-twisting flux tubes on the magnetopause and solar wind particle entry into the magnetosphere, *Geophys. Res. Lett.*, *13*, 801, doi:10.1029/GL013i008p00801.

Schindler, K., M. Hesse, and M. Birn (1988), J. General magnetic reconnection, parallel electric fields, and helicity, *J. Geophys. Res.*, *93*, 5547, doi:10.1029/JA093iA06p05547.

Siscoe, G. L., G. M. Erickson, B. U. Ö. Sonnerup, N. C. Maynard, K. D. Siebert, D. R. Weimer, and W. W. White (2001), Global role of $E_{||}$ in magnetopause reconnection: An explicit demonstration, *J. Geophys. Res.*, *106*, 13,015, doi:10.1029/2000JA000062.

Siscoe, G. L., G. M. Erickson, B. U. Ö. Sonnerup, N. C. Maynard, J. A. Schoendorf, K. D. Siebert, D. R. Weimer, W. W. White, and G. R. Wilson (2002), Flow-through magnetic reconnection, *Geophys. Res. Lett.*, *29*(13), 1626, doi:10.1029/2001GL013536.

Smith, C. W., M. H. Acuna, L. F. Burlaga, J. L'Heureux, N. F. Ness, and J. Scheifele (1981), The ACE magnetic field experiment, *Space Sci. Rev.*, *86*, 613, doi:10.1023/A:1005092216668.

Sonnerup, B. U. Ö. (1970), Magnetic field reconnection in a highly conducting incompressible fluid, *J. Plasma Phys.*, *4*, 207.

Sonnerup, B. U. Ö. (1974), The magnetopause reconnection rate, *J. Geophys. Res.*, *79*, 1546, doi:10.1029/JA079i010p01546.

Sonnerup, B. U. Ö., G. Paschmann, I. Papamastorakis, N. Sckopke, G. Haerendel, S. J. Bame, J. R. Asbridge, J. T. Gosling, and C. T. Russell (1981), Evidence for magnetic field reconnection at the Earth's magnetopause, *J. Geophys. Res.*, *86*, 10049, doi:10.1029/JA086iA12p10049.

Trattner, K. J., S. A. Fuselier, and S. M. Petrinec (2004), Location of the reconnection line for northward interplanetary magnetic field, *J. Geophys. Res.*, *109*, A03219, doi:10.1029/2003JA009975.

Trattner, K. J., S. A. Fuselier, S. M. Petrinec, T. K. Yeoman, C. Mouikis, H. Kucharek, and H. Reme (2005), Reconnection sites of spatial cusp structures, *J. Geophys. Res.*, *110*, A04207, doi:10.1029/2004JA010722.

Trattner, K. J., J. S. Mulcock, S. M. Petrinec, and S. A. Fuselier (2007), Location of the reconnection line at the magnetopause during southward IMF conditions, *Geophys. Res. Lett.*, *34*, L03108, doi:10.1029/2006GL028397.

Tsyganenko, N. A. (1995), Modeling the Earth's magnetospheric magnetic field contained within a realistic magnetopause, *J. Geophys. Res.*, *100*, 5599, doi:10.1029/94JA03193.

Tsyganenko, N. A., and D. P. Stern (1996), Modeling the global magnetic field of the large-scale Birkeland current systems, *J. Geophys. Res.*, *101*, 27,187, doi:10.1029/96JA02735.

White, W. W., G. L. Siscoe, G. M. Erickson, Z. Kaymaz, N. C. Maynard, K. D. Siebert, B. U. Ö. Sonnerup, and D. R. Weimer (1998), The magnetospheric sash and cross-tail S, *Geophys. Res. Lett.*, *25*, 1605, doi:10.1029/98GL50865.

A. Balogh, C. Carr, and E. Lucek, Blackett Laboratory, Imperial College, London, SW7 2BZ, UK.

J. Berchem, Institute of Geophysics and Planetary Physics, University of California Los Angeles, 3877 Slichter Hall, Box 951567, Los Angeles, CA 90095, USA. (jberchem@igpp.ucla.edu)

J. M. Bosqued, I. Dandouras, and H. Reme, Centre d'Etude Spatiale des Rayonnements, UMR 5187, CNRS, 9 Avenue du Colonel Roche, BP 44346, F-31028 Toulouse Cedex 4, France.

M. Dunlop, Rutherford Appleton Laboratory, Didcot OX11 0QX, UK.

C. P. Escoubet, European Space Research and Technology Centre, European Space Agency, Keplerlaan 1, Postbus 299, NL-2200 AG Noordwijk, Netherlands.

A. Marchaudon, Laboratoire de Physique et Chimie de l'Environnement, CNRS, 3A Avenue de la Recherche Scientifique, F-45071 Orléans CEDEX 2, France.

Z. Pu, School of Earth and Space Sciences, Peking University, Building YiFu No. 2, 100871 Beijing, China.